Journal of Empirical Finance 37 (2016) 1–19

Contents lists available at ScienceDirect

Journal of Empirical Finance

journal homepage: www.elsevier.com/locate/jempfin

Bringing an elementary agent-based model to the data: Estimation via GMM and an application to forecasting of asset price volatility☆

Jaba Ghonghadze[a], Thomas Lux[a, b,*]

[a] Department of Economics, University of Kiel, Olshausenstr. 40, 24118 Kiel, Germany
[b] Banco de España Chair in Computational Economics,University Jaume I, Campus del Riu Sec, 12071 Castellon, Spain

ARTICLE INFO

Article history:
Received 15 October 2015
Accepted 2 February 2016
Available online 13 February 2016

JEL classification:
G12
C22
C53

Keywords:
Sentiment dynamics
GMM estimation
Volatility forecasting

ABSTRACT

We explore the issue of estimating a simple agent-based model of price formation in an asset market using the approach of Alfarano et al. (2008) as an example. Since we are able to derive various moment conditions for this model, we can apply generalized method of moments (GMM) estimation. We find that we can get relatively accurate parameter estimates with an appropriate design of the GMM estimator that reduces the biases arising from strong correlations of the estimates of certain parameters. We apply our estimator to a sample of long records of returns of various stock and foreign exchange markets as well as the price of gold. Using the estimated parameters to form the best linear forecasts for future volatility we find that the behavioral model generates sensible forecasts that get close to those of a standard GARCH(1,1) model in their overall performance, and often provide useful information on top of the information incorporated in the GARCH forecasts.

1. Introduction

Asset markets have been known for a long time to be characterized by a set of ubiquitous 'stylized facts' that are hard to explain by any traditional approach to asset pricing. The best known of these are the fat tails of the unconditional distribution of returns and the volatility clustering characterizing their conditional distribution. Known since the 60s, but largely mysterious in terms of their behavioral origins, these salient features have also occasionally been classified as 'anomalies'. However, the latter term appears odd in view of the fact that these are really the constants in the statistical analysis of time series of financial markets across time, countries and asset types, i.e. the imprint of their apparently 'normal' mode of operation.

Under the traditional 'efficient market paradigm' the time series (a)noma-lies are interpreted as the mere reflection of the same (a)nomalies of the 'fundamental factors' of asset prices. However, the fundamentals consist of a conglomerate of diverse factors (macroeconomic, firm-specific, etc.) and as an ensemble they are not observable so that this aspect of the efficient market

☆ We gratefully acknowledge financial support from the European Union's 7th Framework Programme under the grant agreement no. 612955. We are also thankful for helpful comments from Zhenzi Chen, Reiner Franke and from the audience of various seminar and conference presentations.
* Corresponding author at: University of Kiel, Olshausenstr. 40, 24118 Kiel, Germany. Tel.: +49 431 880 3661.
E-mail address: lux@economics.uni-kiel.de (T. Lux).

http://dx.doi.org/10.1016/j.jempfin.2016.02.002
0927-5398/

paradigm cannot be tested directly. While there do not even exist examples of fundamental factors whose time-variation would share the phenomenology of fat tails and clustered volatility, these features could also suggest a more behavioral explanation rather than the mere transmission of information from fundamental factors into changing prices. For instance, 'fat tails' are represented by an unusually high number of extremely large observations which resonates with the notion of excessive volatility of financial markets. Indeed, one of the most convincing components of the body of empirical evidence against the efficient market hypothesis is evidence for excessive volatility according to the test strategy developed first by Shiller (1981). In a similar vein, clustering of volatility could originate from waves of speculative behavior or overoptimism of market participants occasionally switching to overpessimism, 'risk appetite' changing over time, and similar descriptions of financial market turmoil.

The first attempts at explaining the stylized facts with behavioral models have come forth since about the beginning of the 1990s. Examples include Kirman (1991, 1993), De Grauwe et al. (1993), and Lux (1995), among others. While early contributions were targeting phenomena like excessive volatility and endogenous emergence of bubbles and crashes, the subsequent literature has also concentrated on reproducing time series from behavioral market models that could reproduce those of empirical records. Most of this research is conducted via simulation studies, since 'stylized facts' are statistically characterized by higher-order conditional and unconditional moments that for complex models of the market process with heterogeneous agents are hard to derive analytically. Meanwhile, a broad range of models exists that all get close to empirical market behavior or even generate synthetic data that are hard to distinguish with statistical tests from 'real' ones, cf. the surveys by Hommes (2006), LeBaron (2006), Samanidou et al. (2007) and Lux (2008). It appears that the combination of stabilizing and destabilizing (centripedal and centrifugal) forces as represented by, e.g., trend following and chartist strategies, on the one hand, and arbitrage activities based on some perception of an underlying fundamental value by some agents, on the other hand, is generally sufficient to generate a process that with a bit of stochasticity added, is able to provide very realistic data for a broad class of models varying in their exact details. Models in this vein range from simple "zero intelligence" settings (Kirman, 1991; Cont and Bouchaud, 2000) over chartist-fundamentalist models (Lux and Marchesi, 1999; Brock and Hommes, 1998) to models in which agents continuously develop their strategies with some kind of artificial learning algorithm (LeBaron et al., 1999; Lux and Schornstein, 2005).

With this literature having reached a status of consolidation, one natural further research direction is the empirical estimation and validation of such models. This is an endeavor economists are not accustomed to as empirical implementation in an economic context has typically been concerned with (sets of) reduced form equations of behavioral characterizations of representative agent models (expressed, for instance, via the Euler equations characterizing the optimal path of economic activity of such a representative agent). In the present context one would rather have to estimate models with an ensemble of agents with more or less complex interactions. However, there is no fundamental problem involved in such an undertaking. Typical agent-based models can be represented as Markovian stochastic processes and, thus, often generically fulfill a number of 'regularity conditions' that are needed for the application of certain estimation strategies. Relatively simple models might also be amenable to some kind of reduced-form condensation which, in fact, will be the case for the model studied in the following chapters.

Previous attempts of estimation of behavioral or agent-based models of financial markets are sparse. Examples include: Amilon (2008) who estimated the model of Brock and Hommes (1998) by maximum likelihood and efficient method of moments approaches, Gilli and Winker (2003) who attempted to estimate the 'ant' model of Kirman (1993) via nonlinear optimization techniques, Alfarano et al. (2005) who estimated an extended version of the same model via an approximate likelihood approach, and a recent series of papers by Franke and Westerhoff (2011, 2012, 2014) in which a variety of extremely simplified versions of agent-based models are estimated via moment matching approaches. Jang (2013) also uses a simulated method of moments approach for a closely related model, and reports certain principal difficulties in estimating even a very basic agent-based model: He finds the surface of the objective function to be very flat over certain regions so that the chosen moments provide little scope in differentiating between different parameter sets, and he highlights that a very rugged surface of the objective function also makes the search for a global optimum computationally difficult as the danger to get trapped in one out of many local minima of the objective function is hard to assess.

In the present study, we attempt to contribute to this literature by exploring more systematically the issues surrounding the estimation of a prototype agent-based behavioral market model. Our model is of the same class as investigated already by Gilli and Winker (2003), Alfarano et al. (2005) and Jang (2013). Among a number of closely related varieties we choose the specification of Alfarano et al. (2008). The latter has the advantage that the authors have derived already a set of moments that with a bit more of effort can be expanded into moment conditions of an estimable version of their model. These are the basic moments that characterize the stochastic dimension of the stylized facts, i.e. higher moments of returns and autocorrelations of such higher moments. We use these moments in a generalized method of moments (GMM) setting which, due to the absence of simulation in the estimation process, is more transparent than an SMM approach without any analytical input. By and large, we will see that the problems highlighted in previous literature can be overcome with a judicious choice of the moment conditions and the estimation strategy. An empirical application indicates that the present simple model already gets so close to the key moments characterizing fat tails and clustered volatility that it can mostly not be rejected as the underlying data-generating process for these moments even for relatively long data sets extending over several decades. A forecasting exercise demonstrates that the behavioral model possesses significant forecast capacity for short- and medium-term volatility. While its forecast performance remains generally somewhat inferior to that of a baseline GARCH model, it is often not 'encompassed' by the GARCH model, i.e. it adds valuable information on top of that extracted by the GARCH model.

The rest of this paper proceeds as follows. Section 2 introduces the agent-based model and its 'reduced form' representation in the form of a stochastic differential or Langevin equation. Section 3 provides an exposition of the GMM estimation and the moment conditions used. Section 4 provides Monte Carlo results for different specifications of the estimator. Section 5, then,

contains the empirical application, and Section 6 concludes. In an Appendix we provide the details of the derivation of our moment conditions as well as results from an alternative simulation algorithm for the underlying model.

2. An elementary agent-based model of sentiment formation and asset price dynamics

The model investigated in Alfarano et al. (2008) basically extends Kirman's (1993) seminal herding model into a simple asset-pricing model. The overall market consists of fundamental traders as well as those driven by *sentiment* and the time-variation of sentiment is formalized via the herding dynamics. Referring to the second group of agents as noise traders, any one of these at any point in time might be labeled as an optimist or pessimist. The number of agents in an optimistic mood will be denoted by n. With the complete pool of noise traders consisting of N agents, the fraction of optimists at time t, $x_t = (n_t - (N - n_t))/N = 2n_t/N - 1$ can be denoted the current configuration of the sentiment-driven part of the market. Agents' mood might, of course, change over time, and so an optimistic noise trader might become pessimistic and vice versa. This happens with transition rates $\pi_{\downarrow,t}$ and $\pi_{\uparrow,t}$ in continuous time. Transitions consist of an autonomous part for idiosyncratic changes of opinion and an "interactive" part driven by interpersonal communication:

$$\pi_{\uparrow,t} = a + \frac{n_t}{N} b = a + \frac{1}{2} b(1 + x_t), \tag{1}$$

$$\pi_{\downarrow,t} = a + \frac{N - n_t}{N} b = a + \frac{1}{2} b(1 - x_t). \tag{2}$$

Here a is the propensity to change one's opinion due to idiosyncratic reasons (as a rate per time unit) and b is the propensity to change one's opinion under the influence of an agent of the other group (again as a rate per time unit). To meet one person with an antagonistic opinion happens with a probability proportional to n_t/N for a pessimist and $(N - n_t)/N$ for an optimist which defines the second part of both equations ($\uparrow$ denotes switch of a pessimist to optimist and the reverse for $\downarrow$). Population transition rates ($\omega_{\uparrow,t}$ and $\omega_{\downarrow,t}$) are then simply obtained by multiplying the individual ones by the respective number of agents, and are, thus, obtained as:

$$\omega_{\uparrow,t} = (N - n_t)\left(a + b\frac{n_t}{N}\right) \tag{3}$$

$$\omega_{\downarrow,t} = n_t\left(a + b\frac{N - n_t}{N}\right). \tag{4}$$

Technically, this is a system of Poisson processes (one for each agent) with transition rates being linear and state-dependent. Such systems have also been denoted as jump Markov processes (cf. Aoki, 2002).

The configuration of sentiment, x_t, is embedded into an asset pricing framework by assuming that optimistic (pessimistic) agents will buy (sell) a fixed volume of shares T_c. In addition, there is another component of excess demand composed of fundamentalists who are sensitive to deviations between the log market price, p_t, and their assumed log fundamental value, $p_{f,t}$.

Price adjustments are assumed to occur in the usual Walrasian manner in the presence of excess demand. Combining these aspects we arrive at the price adjustment equation:

$$\frac{dp}{dt} = \beta\left(T_f\left(p_{f,t} - p_t\right) + NT_c x_t\right). \tag{5}$$

Assuming instantaneous adjustment to market equilibrium, i.e. letting the price adjustment speed $\beta \to \infty$, we obtain:

$$p_t = p_{f,t} + \frac{NT_c}{T_f} x_t \tag{6}$$

which shows how sentiment may trigger deviations from fundamental valuation.

Returns over finite time increments (e.g., daily returns) can be written as:

$$r_t = p_{t+1} - p_t = p_{f,t+1} - p_{f,t} + \frac{NT_c}{T_f}(x_{t+1} - x_t) \tag{7}$$

and, hence, are driven by innovations in the fundamentals and innovations in the sentiment dynamics. We assume that the (log) fundamental value follows Brownian motion with a variance σ_f^2 so that its changes can be written as:

$$p_{f,t+1} - p_{f,t} = \sigma_f \varepsilon_t, \quad \varepsilon_t \sim N(0,1). \tag{8}$$

So far, we have a macroscopic equation for the price combined with the result of the interaction of N agents, x_t. However, the microscopic dynamics of x_t can as well be transformed into a macroscopic process equation. In particular, it can be shown that the transient probability density of x_t, $p(x, t)$, follows a Fokker–Planck or forward Kolmogorov equation:

$$\frac{\partial p(x,t)}{\partial t} = \frac{\partial}{\partial x}A(x)p(x,t) + \frac{1}{2}\frac{\partial^2}{\partial x^2}(D(x)p(x,t)) \tag{9}$$

with drift $A(x, t) = -2ax_t$ and diffusion $D(x, t) = 2b(1 - x_t^2) + 4a/N$. As a consequence, the macroscopic dynamic process can be approximately characterized by a continuous-time diffusion:

$$d\tilde{x}_t = A(\tilde{x}_t) + \sqrt{D(\tilde{x}_t)}dB_t \tag{10}$$

i.e. a diffusion process that 'shares' the same forward Kolmogorov equation with the agent-based process (cf. Lux, 1998; Ethier and Kurtz, 1986, for more details). It is this diffusion process as the reduced-form of our agent-based model that together with the price process, Eq. (6), will be used to derive a set of moment conditions to be used in our subsequent GMM estimation. In Appendix A3 we also provide details of an exact algorithm for simulating the agent-based sentiment process as a discrete event system. We observe that our GMM approach (detailed in the next section) shows virtually the same performance irrespective of whether the underlying sentiment data are obtained via the diffusion approximation or the dicrete exact simulation. This confirms that the former approximation and the moments derived from it are sufficiently close approximations to the original system of Eqs. (1) and (2) and its moments for estimation purposes.

3. Estimation

We will assume throughout that we are given equidistant observations of market prices, p_{t_i}, $t_i = \Delta t i$, $i = 0, \ldots, t$, making a sample of size $(T + 1)$. We calculate from Eqs. (6), (7) and (8)

$$r_t = \sigma_f \varepsilon_t + \frac{NT_c}{T_f}(x_{t+1} - x_t), \tag{11}$$

where ε_t is a standard normal variate that is independent from x_t at all lags. Thus, we observe a sequence of the log-returns r_t of size T. The parameter vector θ to be estimated is $\theta := (a, b, \sigma_f)'$. Note that we do not estimate the parameters N, T_c, and T_f. We assume that these are given by $N = 100$, and $NT_c/T_f = 1$. Given that these three parameters enter in a multiplicative way, we could at best hope to estimate N (which also enters the diffusion function of the reduced-form equation of the sentiment process), and T_c/T_f. However, preliminary investigations showed that when including these as free parameters, the problems of weak identification reported below for the remaining ones will become paramount. Essentially, with these parameters entering as pre-factors for $z_t \equiv x_{t+1} - x_t$, they are so close to colinear with a, the drift factor of the diffusion process, that with limited data, their separate estimation becomes impossible. Nevertheless, inspection of the moment conditions derived below immediately indicates that with a sufficient number of moment conditions used, also for a 5-parameter model $\tilde{\theta} = (a, b, \sigma_f, N, T_c/T_f)$ identification in the strict sense does hold, and so with an infinite supply of data one would be able to estimate these parameters.

3.1. The GMM procedure

We use θ to denote an arbitrary element of the three dimensional parametric space Θ and let θ_0 to be the true parameter vector. The GMM procedure due to Hansen (1982) requires to formulate a number $q \geq 3$ moment conditions, $m_t = [m_{1t}, \ldots, m_{qt}]'$. Here, we will be using simple unconditional moment conditions like:

$$m_{1t} = r_t^2 \tag{12}$$

$$m_{2t} = r_t^4 \tag{13}$$

$$m_{3t} = r_t^2 r_{t-1}^2 \tag{14}$$

and higher lags of the autocovariances of squared returns. Their sample counterparts are $M_T = [M_{1T}, \ldots, M_{qT}]'$, where

$$M_{iT} = \frac{1}{(T-k)}\sum_{t=k+1}^{T} m_{it}$$

for all i from the set $\{1, \ldots, q\}$ and k defines the maximum lag between the variables that enter the sample moments.

Denote the corresponding q-dimensional vector of analytic moments, $m(\theta) := [m_1(\theta), \ldots, m_q(\theta)]'$ such that

$$\mathbb{E}[m_t(\theta)] = m(\theta).$$

It is customary to introduce a vector-valued function $g_T(\theta) := M_T - m(\theta)$ which besides θ depends also on the T-dimensional data vector $\mathbf{r}_T$ through M_T.

The GMM estimator, $\hat{\theta}_T$, minimizes the distance between $m(\theta)$ and M_T over the parametric space Θ in the following quadratic form,

$$Q(\theta)_T := g_T(\theta)' W_T g_T(\theta), \tag{15}$$

where W_T is a positive semi-definite matrix which may depend on the data but converges in probability to a positive definite matrix of constants (Hall, 2005, see p. 14). That is,

$$\hat{\theta}_T = \arg\min_{\theta \in \Theta} Q(\theta)_T. \tag{16}$$

The GMM theory does not give recommendations on the optimal selection of the moment conditions. In practice, this choice is up to the researcher. However, the theory provides information on the optimal choice of the weighting matrix in the sense that it leads to an estimator with the smallest asymptotic errors. In particular, if Ω denotes the asymptotic covariance matrix of the moment conditions (to be specified below), then choosing $W = \Omega^{-1}$ gives us the sought efficient weighting matrix. Let $g_t(\theta) := m_t(\theta) - m(\theta)$ and consider $D := \mathbb{E}[\partial g_t(\theta_0)/\partial \theta']$. Then, under appropriate regulatory conditions, $\hat{\theta}_T$ is consistent and $\sqrt{T}\left(\hat{\theta}_T - \theta_0\right)$ is asymptotically normal with mean zero and covariance matrix $V := D'WD$, that is, $\sqrt{T}\left(\hat{\theta}_T - \theta_0\right) \xrightarrow{d} \mathcal{N}(0, V)$.

Following most of the extant GMM literature, we have adopted the standard Newey–West estimation of the covariance matrix, and used an iterative GMM scheme, i.e. we computed a new estimate of the covariance matrix based upon the estimated set of parameters in each round and iterated the sequence of GMM estimations until convergence of the parameter estimates was obtained.

3.2. The moment conditions

The moment conditions that are available by appropriate extension of the results of Alfarano et al. (2008) are basically various powers of returns and their covariances. Among the unconditional powers, odd moments are uninteresting as they are mostly close to zero both in the empirical data and in the analysis of our model.[1] Flat or almost flat moments are, however, not informative and would presumably increase the uncertainty of parameter estimates and distort the size of the J test for accurate matching of the moments used. Since higher powers also become increasingly noisy, the most practical choice is to use squared returns and the fourth moment. Theoretical approximations of autocovariances can be obtained for squared returns over arbitrary time lags while again, autocorrelations of odd powers would not be very informative and autocovariances of higher powers than the second would be very hard to obtain, and perhaps also very noisy. Thus, we are basically depending on the most elementary measurements of the stylized facts for our GMM implementation: Kurtosis and autoregressive dependency of squared returns. For univariate time series of asset prices, this is essentially the "portfolio" of moments for GMM or SMM estimation. Note that some authors (e.g. Franke and Westerhoff, 2012, 2014) have used more refined measures such as the tail index for the decay of the density of the unconditional distribution, or similar measures for the decay of the autocorrelation function. While GMM/SMM based on such more complicated objects derived from the data is perfectly legitimate, a certain backdrop is that an efficient estimate of the covariance matrix of these moment conditions is not easy to define. Hence, one has to sacrifice efficiency compared to a potentially optimal estimator. We, therefore, try to incorporate such information in a somewhat different format into a standard GMM framework. We do so by not just considering single autocovariances $r_t^2 r_{t-h}^2$ but rather sums of these: $\sum_{h=t_1}^{T_1} r_t^2 r_{t-h}^2$ as these sums characterize the curvature over a certain range of lags and might, therefore, give less noisy information than single autocovariances. Such moments might actually convey structural information equivalent to the decay rate of the ACF. The use of such sums of moments is perfectly in line with the GMM framework and we will explore their effectiveness in the next section.

Now let us turn to the exact moment conditions. Starting with the second moment, we easily find that

$$\mathbb{E}\left[r_t^2\right] = \sigma_f^2 + \mathbb{E}\left[(x_{t+1} - x_t)^2\right] = \sigma_f^2 + \mathbb{E}\left[z_t^2\right] = \sigma_f^2 + 2\mathbb{E}\left[x_t^2\right]\left(1 - e^{-2a}\right) \tag{17}$$

with $z_t = x_{t+1} - x_t$ and

$$\mathbb{E}\left[x_t^2\right] = \frac{b}{b + 2a}. \tag{18}$$

[1] In simulations, we find the small autocorrelation of raw returns at lag 1 imposed by the bounded variation of the sentiment dynamics to be practically indistinguishable from zero, i.e. the sampling standard error exceeded the estimated autocorrelation by far, even for large samples.

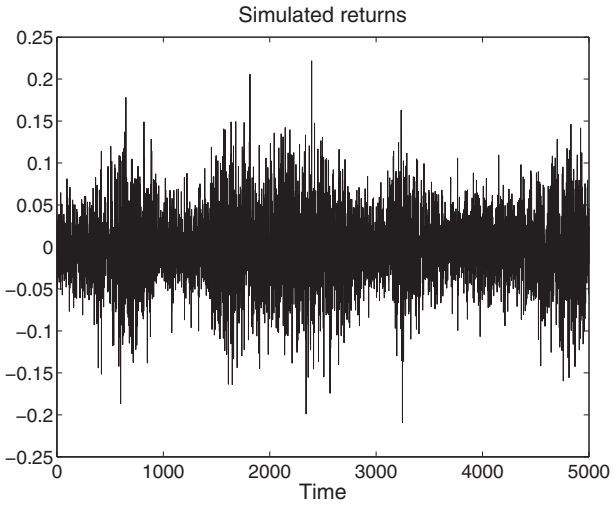

Fig. 1. Typical simulation with parameter set θ.

Moving on to the fourth moment, it is also easy to see that:

$$\mathbb{E}\left[r_t^4\right] = 3\sigma_f^4 + 6\sigma_f^2\mathbb{E}\left[z_t^2\right] + \mathbb{E}\left[z_t^4\right]. \tag{19}$$

We can derive $\mathbb{E}[z_t^4]$ as follows (cf. the Appendix):

$$\mathbb{E}\left[z_t^4\right] = 8\mathbb{E}\left[x_t^4\right]\left\{\frac{a+b}{2a+b} - e^{-2a} + \frac{a}{2a+b}e^{-2(2a+b)}\right\} \tag{20}$$

and

$$\mathbb{E}\left[x_t^4\right] = \frac{3b}{2a+3b}\mathbb{E}\left[x_t^2\right]. \tag{21}$$

Finally, autocovariances of squared returns are defined as

$$\mathbb{E}\left[r_t^2 r_{t-h}^2\right] = \sigma_f^4 + 2\sigma_f^2\mathbb{E}\left[z_t^2\right] + \mathbb{E}\left[z_t^2 z_{t-h}^2\right] \tag{22}$$

where we show again in the Appendix that

$$\mathbb{E}\left[z_t^2 z_{t-h}^2\right] = 4b^2(1-2(2a+b))^{h-1}\left(\mathbb{E}\left[x_t^4\right] - \mathbb{E}\left[x_t^2\right]^2\right) + \mathbb{E}\left[z_t^2\right]^2. \tag{23}$$

4. Monte Carlo results

In order to assess the quality of the proposed GMM estimator, we have conducted a series of Monte Carlo experiments.

In the baseline setting, we assume that the log returns follow Wiener Brownian motion without drift. The fundamental dynamics is, thus, simply characterized by its standard deviation σ_f. We choose the parameter set $\theta = (a, b, \sigma_f) = (0.0003, 0.014, 0.03)$ together with the number of agents $N = 100$. This is a parameter set in the vicinity of typical empirical estimates, and it satisfies a number of conditions: (i) it generates data that is roughly in line with the empirical appearance of financial returns featuring fat tails and clustering of volatility, see Fig. 1, (ii) it has roughly equal contributions of the fundamental changes and the sentiment component to the overall variation of asset prices (which appears to be a good starting point), (iii) it enables us to approximate the underlying agent-based model by its associated Langevin equation to a reasonable degree of accuracy. We simulate the Langevin equation with time increments $\Delta t < \frac{2}{N(2a+bN)}$ that guarantee that the sum of all transition probabilities remains smaller than 1. Since the parameter set θ leads to a bimodal outcome of the sentiment process, we

Table 1
Sensitivity of Moments to Parameter Changes.

	m_1	m_2	m_3	m_4	m_5	m_6	m_3'	m_4'
Parameter set I								
a	0.079	0.136	0.136	0.136	0.136	0.136	0.136	0.137
b	0.121	0.329	0.329	0.328	0.328	0.327	0.316	0.293
σ_f	0.412	0.889	0.889	0.889	0.889	0.888	0.888	0.889
Parameter set II								
a	0.007	0.014	0.014	0.014	0.014	0.014	0.014	0.014
b	0.094	0.197	0.197	0.197	0.197	0.197	0.197	0.196
σ_f	0.445	1.087	1.087	1.087	1.087	1.087	1.087	1.087

Notes: The table displays calculations of the sensitivity of the six moment conditions with respect to parameter variations. Changes by 25% of each one of the parameters have been considered. The moments we have used are in their order of appearance in the table: squared returns, the fourth moment and autocovariances of squared returns at lags 1, 5, 10 and 20, as well as the sums of autocovariances over lags 1 through 50 (m_3') and 51 through 100 (m_4'), respectively.

have also conducted Monte Carlo runs for a case with uni-modal dynamics given by the parameter set $\theta' = (0.014, 0.0003, 0.03)$. Baseline GMM results are documented as "GMM1" in Tables 1 and 2. The moments we have used are squared returns, as well as their fourth moment and autocovariances of squared returns at lags 1, 5, 10 and 20. Table 1 shows that our chosen moment conditions display sufficient variation when changing the parameters around θ and θ' so that the underlying parameters should

Table 2
Monte Carlo results for GMM estimation of ALW Model.

True:	0.3	1.4	30	0.3	1.4	30	0.3	1.4	30
	GMM1			GMM2			GMM3		
	a	b	σ_f	a	b	σ_f	a	b	σ_f
T = 5000									
Mean	0.433	1.178	28.617	0.371	1.238	28.746	0.354	1.328	29.604
FSSE	0.251	0.531	5.392	0.236	0.300	5.481	0.218	0.315	6.246
RMSE	0.284	0.575	5.560	0.247	0.341	5.616	0.225	0.323	6.250
T = 10,000									
Mean	0.406	1.119	28.944	0.297	1.304	30.054	0.294	1.393	30.671
FSSE	0.203	0.510	4.970	0.098	0.286	4.178	0.100	0.277	4.684
RMSE	0.228	0.582	5.075	0.098	0.301	4.173	0.100	0.276	4.726
T = 20,000									
Mean	0.409	1.064	28.999	0.275	1.469	31.290	0.271	1.494	31.682
FSSE	0.226	0.447	5.320	0.082	0.207	3.130	0.069	0.201	2.762
RMSE	0.250	0.559	5.407	0.086	0.218	3.382	0.075	0.222	3.231
True:	1.4	0.3	30	1.4	0.3	30	1.4	0.3	30
	GMM1			GMM2			GMM3		
	a	b	σ_f	a	b	σ_f	a	b	σ_f
T = 5000									
Mean	0.895	0.641	28.119	1.064	0.446	27.419	1.111	0.446	27.256
FSSE	0.441	0.548	2.387	0.194	0.024	0.830	0.191	0.010	0.367
RMSE	0.670	0.645	3.037	0.388	0.148	2.710	0.347	0.146	2.769
T = 10,000									
Mean	0.930	0.683	27.818	1.107	0.448	27.324	1.146	0.446	27.263
FSSE	0.440	0.597	2.679	0.111	0.008	0.339	0.206	0.010	0.288
RMSE	0.644	0.709	3.453	0.313	0.148	2.697	0.327	0.146	2.752
T = 20,000									
Mean	1.057	0.634	27.312	1.124	0.448	27.301	1.182	0.445	27.232
FSSE	0.384	0.550	2.861	0.103	0.006	0.163	0.235	0.009	0.252
RMSE	0.515	0.642	3.923	0.295	0.148	2.704	0.321	0.146	2.780

Notes: The table shows the means, finite sample standard errors (FSSE) and root-mean squared errors (RMSE) of 400 replications of each scenario. Estimated parameters are multiplied by 10^3 for better readability. GMM1 stands for a standard GMM estimation, while in GMM2 the estimation has been initiated with the inverse of the variance–covariance matrix of the test data as the weighting matrix in the first step of the estimation. In GMM3, single autocovariances have been replaced by sums of autocovariances.

be guaranteed to be identified. Note, however, that the fourth moment as well as the autocovariances m_3 through m_6 show very homogeneous variation under variations of our parameters. This might imply that adding more moments hardly leads to higher precision of our estimates.

Since this is a nonlinear model with possibly multiple local minima of the objective function, and we would not have any clear ex-ante perception on the range of "realistic" parameter values in an empirical application, we have first conducted a grid search in the admissible parameter space and have subsequently initiated the GMM estimation from the 10 best out of 9^3 grid points. These grid points have been chosen equidistantly along all three dimensions: given the variance of each set of test data, we have chosen σ_f so that the fundamental variation would account for 0.1, 0.2, . . ., 0.9 of the total sample variance. Given the grid value of σ_f, a and b have been varied around the bifurcation value $\epsilon_0 = a/b$ over 9 equidistant points each with center at ϵ_0 and four points to its right and left within the unimodal and bimodal regimes. The exact location of the grid points of a and b has also been chosen for each sample to bring them into rough agreement with the sample variance.

We have used sample sizes of 5000, 10,000 and 20,000 observations. Results are to be found under the heading 'GMM1' in Table 2. While our estimates are centered in the vicinity of their 'true' values, and for a and b show roughly declining biases with increasing sample size, the overall quality of the estimates appears to show no significant improvement with higher sample sizes — their finite sample standard errors (FSSE) and root mean-squared errors (RMSEs) are about the same for all sample sizes. This behavior is puzzling as our process should meet all standard "regularity" conditions required for GMM estimation, and the chosen six moments should allow identification of the parameters. Note that our moment conditions are nonlinear in all parameters so that identification should be generic (cf. McManus, 1992). Upon closer inspection, we find that our parameter estimates suffer from a particularly high correlation between σ_f and a that leads to a certain number of outliers. The reason is that these variables are somewhat complementary in that they determine the variances of the fundamental and sentiment component (while the sentiment variance depends on both a and b, the behavior of the estimates actually shows that a is more relevant for the variance of the process). Thus, changing σ_f and a in opposite directions roughly leaves the second moment intact. While this might effect autocovariances, changes of b might also bring those closer to the theoretical moments. As a consequence, we find a certain number of runs that get stuck in local minima.

Note also that in the grid search and initialization we have used unweighted moments (or weighted by the identity matrix — the default initialization of a routine GMM estimation). In the present setting, the second moment will be much larger in absolute value than the fourth moments and the autocovariances of squared returns. Hence, to not let the second moment exert an all-dominating influence in the first step and to bias to one side the overall results, it could be useful to already use some information on the precision of different moments in the first step. To this end, we have computed a weighting matrix that is the inverse of the variance–covariance matrix of the moments in the test data. Using this unconventional initialization (for both the grid search and the first iteration of the GMM) we indeed find a uniform improvement of our results in the more realistic parameter set θ. The pertinent outcome is summarized under the heading "GMM2" in Table 2. As it turns out, the performance of this alternative estimator beats that of the conventional one in all respects under parameter set θ: FSSEs and RMSEs are always smaller than with GMM1 (particularly so for a and b where the FSSEs and RMSEs are only about 50% of those of GMM1), and the precision of the estimates becomes recognizably better with increasing sample size. For θ', we find a strong improvement in the quality of the estimates of all parameters. In this case, however, higher accuracy with increasing sample size is confined to parameter a. Figs. 2 and 3 show histograms of the parameter estimates of parameter set θ across the 400 Monte Carlo runs and provide additional illustrations of the distortive effects explained above which are still present (though less pronounced) in the results from GMM2.

Table 3 exhibits the population correlation matrices of the 400 Monte Carlo runs of Table 2. The dominating feature is the strong negative correlation between a and σ_f across all sample sizes. Note that this entry is even increasing with sample size which shows that with generally more precise estimates for higher T this distortive feature explains even more of the deviation from the 'true' values. In contrast, the two parameters of the sentiment process are virtually uncorrelated while b and σ_f are moderately positively correlated. Presumably, this shows that a higher estimate of the fundamental variance has to be compensated by more pronounced herding to match the volatility clustering measured by the autocovariances of second moments. Fig. 2 shows how this effect leads to a right-skewed distribution of the estimates of a and a left-skewed distribution for the estimates of σ_f. The distortion due to this near-colinearity trickles away with increasing sample size showing that indeed the parameters are well identified asymptotically. Note that while the overall distribution of the estimates becomes more narrow with larger sample size, there is still a number of outliers. These become relatively more important compared to the mere volatility of the estimates (despite becoming fewer in absolute numbers) which explains the increase of the correlation documented in Table 3. Fig. 3 shows that also the distribution of the estimates of parameter b suffers from skewness, but also here higher precision is attained with higher sample size. Also shown in Fig. 3 is the distribution of the J test statistic for the goodness-of-fit of the moments which appears to be quite different from its asymptotic distribution (displayed as a solid curve). This suggests that based on our moment conditions the J test would reject too often the null hypothesis of equality of sample and theoretical moments.

Can we do any better with our limited information on these key unconditional and conditional statistics by using information aggregated over many lags as incorporated in moments m_3' and m_4' (thus, extracting information on the decay of volatility autocorrelation)? Table 2 lists as GMM3 a setting with four moments only, where, however, the conditional moments are sums of autocovariances, i.e. $m_3' = \sum_{i=1}^{50} r_t^2 r_{t-i}^2$, $m_4' = \sum_{i=51}^{100} r_t^2 r_{t-i}^2$, while m_1 and m_2 again denote the second and fourth conditional moments. We see that this change hardly affects the quality of the estimates. It, thus, appears that a limited set of autocorrelations of squared returns suffices to extract what information lies in the temporal dependence structure of the second

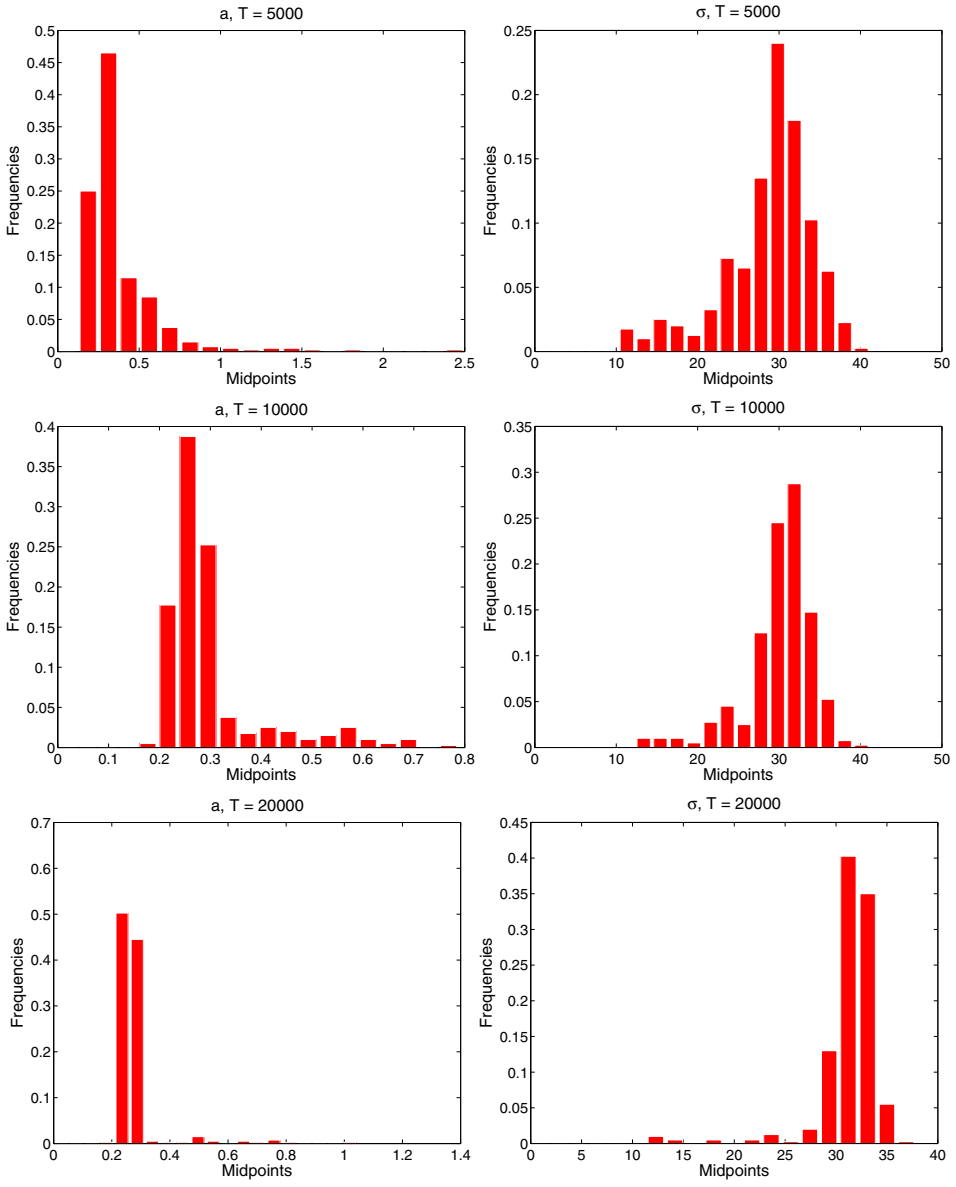

Fig. 2. Distribution of parameter estimates a and σ_f. Note: The underlying data set is $\theta = (0.0003, 0.014, 0.03)$.

moment. Graphical representations of the Monte Carlo results from GMM3 look very similar to those of GMM2 depicted in Figs. 2 and 3.

A cumbersome feature one finds in Table 2 is that for parameter vector θ' the Monte Carlo results show little indication of improving from sample sizes $T = 5000$ to $T = 10,000$ or $T = 20,000$ under GMM2 and GMM3, particularly for parameter b. So while overall one obtains relatively precise estimates in these settings compared to GMM1, these typical sample sizes do seem to be far away from the realm of the asymptotic distribution of the estimates, and more data within this range do not lead to significantly better estimates.

Table 7 in Appendix provides results for the same estimation exercise as in Table 2 but with the underlying data extracted from an exact discrete event simulation of Eqs. (1) and (2) together with the process (7) governing returns. Results are virtually identical which confirms the quality of the diffusion approximation and its moments in capturing the aggregate dynamics of the agent-based model.

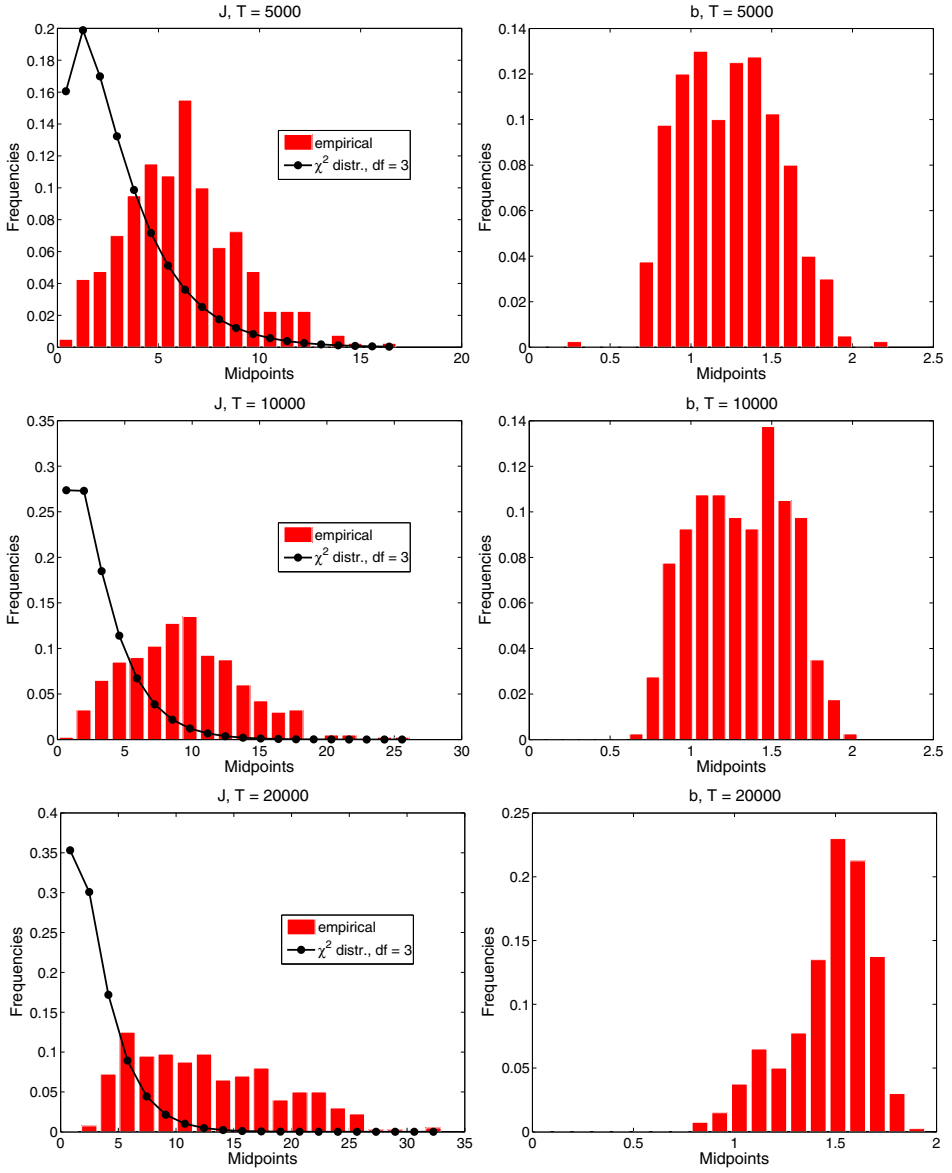

Fig. 3. Distribution of parameter b and J test statistics. Note: The underlying Parameter set is $\theta = (0.0003, 0.014, 0.03)$. The J test statistics is shown together with its asymptotic χ^2 distribution.

5. An empirical application

Given the acceptable performance of our modified GMM estimates, we turn to an empirical application. We have selected a number of important financial indices and other assets to explore the performance of our model. Table 4 exhibits estimation results for three stock market indices, three exchange rates and the price of gold. The stock market indices are: the S & P 500, the German DAX and the Japanese Nikkei. For these series and for the gold price, we have used daily data from the start of 1980 until the end of the year 2004, a total of exactly 25 years. The foreign exchange markets are represented by the exchange rates of the Euro against the U.S. dollar (USD/EUR) and against the Swiss franc (CHF/EUR) as well as the Japanese yen against the U.S. dollar (YEN/USD). Data for these series include the periods 01/01/1999 to 12/31/2009 (USD/EUR), 7/15/2003 to 12/31/2009 (CHF/EUR) and 1/1/1986 to 12/31/2004 (YEN/USD). Since due to the introduction of the Euro in 1999, the two exchange rates involving this currency have a shorter history, we have extended the pertinent samples by five years until the end of 2009. Table 4 shows results for both the GMM2 and GMM3 algorithms. Interestingly, we find that the results from both sets of moments are mostly very close to each other with particularly the parameter σ_f often being undistinguishable. The later finding indicates that the

Table 3
Correlation Matrices of GMM Estimates.

	a	b	σ_f
T = 5000			
	1.000	−0.044	−0.559
	−0.044	1.000	0.542
	−0.559	0.542	1.000
T = 10,000			
	1.000	−0.209	−0.618
	−0.209	1.000	0.593
	−0.618	0.593	1.000
T = 20,000			
	1.000	−0.026	−0.732
	−0.026	1.000	0.449
	−0.732	0.449	1.000

Notes: The table shows the population correlation matrices of the parameter estimates from GMM2 of the 400 replications of each scenario summarized in Table 2.

level of fundamental noise is mainly extracted from the second and fourth unconditional moments (since these are represented in both estimations), while autocovariances are more exploited for the determination of a and b.

As the sentiment dynamics is responsible for volatility clustering, the estimations indeed sensibly decompose the relationships between parameters and moments. Inspecting the estimation results in Table 4 one observes that the estimates of a, b and σ_f have about the same order of magnitudes, respectively, for most of the seven assets under consideration (with the exception of exchange rates against the U.S. dollar). The estimation, thus, typically converges to very similar configurations. In all cases except for the USD/EUR exchange rate under the GMM2 approach we find $b > a$ indicating a bimodal distribution of the underlying sentiment dynamics.

Table 4
Empirical Parameter Estimates.

	GMM2					**GMM3**				
Assets	J	a	b	σ_f	Rel.var	J	a	b	σ_f	R.var
DAX										
	3.963	0.026	0.315	8.368	0.561	5.907	0.026	0.315	8.368	0.561
	(0.266)	(0.003)	(0.033)	(0.995)		(0.015)	(0.013)	(0.080)	(2.189)	
S & P 500										
	2.357	0.016	0.098	6.597	0.528	1.439	0.016	0.131	6.597	0.544
	(0.502)	(0.001)	(0.002)	(0.505)		(0.230)	(0.094)	(0.197)	(17.862)	
Nikkei										
	5.567	0.024	0.191	7.948	0.547	4.874	0.046	0.143	5.487	0.789
	(0.135)	(0.002)	(0.006)	(0.699)		(0.027)	(0.042)	(0.024)	(5.666)	
USD/EUR										
	12.456	0.000	0.000	5.594	0.009	3.599	0.006	0.024	4.448	0.448
	(0.006)	(0.000)	(0.000)	(0.149)		(0.058)	(0.000)	(0.001)	(0.209)	
YEN/USD										
	11.468	0.000	0.062	6.381	0.036	6.762	0.030	0.031	2.273	0.887
	(0.009)	(0.000)	(0.000)	(0.139)		(0.009)	(0.002)	(0.005)	(1.234)	
CHF/EUR										
	1.544	0.001	0.023	1.701	0.639	2.541	0.001	0.020	1.701	0.635
	(0.672)	(0.000)	(0.000)	(0.265)		(0.111)	(0.000)	(0.000)	(0.394)	
GOLD										
	4.105	0.021	0.332	5.263	0.726	6.168	0.021	0.208	5.263	0.713
	(0.250)	(0.004)	(0.061)	(1.253)		(0.013)	(0.008)	(0.056)	(1.861)	

Notes: The table shows parameter estimates in-sample for selected stock market indices, foreign exchange rates, and the price of gold together with the value of Hansen's test of overidentification restrictions (J). Standard errors and the p-value of the test are given in parentheses. The last column shows the relative contribution of the sentiment dynamics to the volatility of returns (measured by its variance).

Table 5
Out-of-Sample Forecast Comparison.

		RMSE	RMSE				RMSE
Data	h	ALW	GARCH	p(DM)	λ	Std. error	f^*
DAX							
	1	0.896	0.866	0.824	0.148	0.068	0.844
	5	0.880	0.862	0.842	0.118	0.116	0.862
	10	0.903	0.884	0.928	0.031	0.126	0.884
	20	0.963	0.945	0.890	0.053	0.136	0.946
	30	0.993	0.963	0.936	−0.188	0.129	0.962
	40	1.028	0.992	0.952	−0.162	0.118	0.992
	50	1.050	1.007	0.964	−0.141	0.107	1.007
S & P 500							
	1	0.871	0.764	0.991	−0.119	0.056	0.758
	5	0.823	0.767	0.984	−0.289	0.089	0.763
	10	0.857	0.817	0.899	−0.138	0.097	0.815
	20	0.910	0.883	0.812	−0.007	0.110	0.882
	30	0.957	0.941	0.828	0.134	0.120	0.939
	40	0.996	0.985	0.754	0.220	0.126	0.982
	50	1.020	1.003	0.779	0.121	0.126	1.001
Nikkei							
	1	0.917	0.778	0.961	0.131	0.041	0.784
	5	0.907	0.880	0.671	0.347	0.053	0.858
	10	0.938	0.944	0.471	0.491	0.055	0.908
	20	0.997	1.108	0.158	0.950	0.058	0.997
	30	1.020	1.161	0.135	1.083	0.058	1.019
	40	1.036	1.204	0.127	1.200	0.059	1.032
	50	1.043	1.223	0.119	1.252	0.059	1.036
USD/EUR							
	1	0.956	0.935	0.984	0.128	0.144	0.931
	5	0.947	0.935	0.895	0.170	0.181	0.932
	10	0.949	0.940	0.788	0.213	0.186	0.936
	20	0.951	0.944	0.744	0.201	0.198	0.940
	30	0.953	0.949	0.660	0.273	0.209	0.945
	40	0.957	0.958	0.458	0.445	0.219	0.952
	50	0.958	0.958	0.497	0.398	0.229	0.953
YEN/USD							
	1	0.967	0.919	0.978	−0.126	0.096	0.919
	5	0.963	0.932	0.963	−0.085	0.115	0.932
	10	0.966	0.935	0.951	−0.176	0.124	0.935
	20	0.978	0.963	0.849	0.115	0.136	0.962
	30	0.986	0.977	0.823	0.258	0.138	0.975
	40	0.992	0.985	0.792	0.327	0.135	0.982
	50	0.996	0.989	0.761	0.345	0.130	0.986
CHF/EUR							
	1	0.995	1.003	0.404	0.513	0.107	0.981
	5	1.012	1.048	0.080	2.018	0.257	1.001
	10	1.015	1.046	0.134	2.261	0.304	1.002
	20	1.017	1.034	0.127	2.723	0.465	1.006
	30	1.002	1.004	0.259	0.270	0.943	1.002
	40	1.002	1.002	0.451	−0.268	0.886	1.001
	50	1.004	1.004	0.562	−0.452	0.788	1.002
GOLD							
	1	0.944	0.926	0.886	0.392	0.135	0.937
	5	0.940	0.938	0.661	0.558	0.312	0.939
	10	0.948	0.946	0.668	0.516	0.313	0.947
	20	0.956	0.956	0.436	0.892	0.312	0.956
	30	0.973	0.972	0.530	0.760	0.310	0.972
	40	0.981	0.980	0.624	0.574	0.305	0.981
	50	0.996	0.994	0.578	0.617	0.300	0.995

Notes: The table shows root-mean squared errors of volatility forecasts for selected assets on the base of the estimated ALW and a standard GARCH(1,1) model. p(DM) denotes the probability of the null hypothesis that both models have the same forecast accuracy against the alternative of better forecast accuracy of the ALW based predictions under the common Diebold–Mariano test. λ is the estimate of the encompassing test with its standard error following in the subsequent column. f^* denotes the relative RMSE of the optimal combination of GARCH and ALW. h stands for the forcasting horizon.

The other exchange rates (CHF/EUR and YEN/USD) are somewhat unusual in that they are characterized by very small values of a indicating a very small noise factor in the sentiment process. The J statistics accepts the model as a possible data generating process for the selected moments at any traditional level of significance except for the two exchange rates USD/EUR and YEN/USD under GMM2. It is more critical under GMM3 where we find non-rejection at the 5% confidence level only for S & P 500, USD/EUR and CHF/EUR. The last column of the Table exhibits the percentage of the return volatility that according to the estimated parameters would be attributed to sentiment changes.[2] We observe numbers in the range between 50 and 70% for most assets and very similar results under GMM2 and GMM3. Only the exchange rates against the U.S. dollar show deviations from this pattern and non-homogeneous outcomes under GMM2 and GMM3.

To just estimate parameters of a model does, however, not yet provide much evidence on its closeness to the behavior of certain data. We, therefore, were interested to compare the ALW model to a standard econometric model for financial returns, the GARCH model of Bollerslev (1986). This is certainly the most common of all volatility models proposed in the literature, and it is well-known that it captures to a large extent the time-varying dynamics of financial volatility. While dozens if not hundreds of extensions exist that add features like asymmetry and long-term dependence we stick to the basic GARCH (1,1) model for comparison basically because it has the same number of parameters (3) like the agent-based model (denoted as ALW model in the following), and because we would not expect our simple model to be a coequal competitor for the most refined econometric models. We compare ALW and GARCH (1,1) by an out-of-sample forecasting exercise: To this end, we take the samples defined above as in-samples for parameter estimation, and use both models to generate out-of-sample forecasts of daily volatility for the remaining available data until the end of February 2015 (i.e. data from either the beginning of 2005 or 2010 to the end of 2/2015). We forecast daily volatility (proxied by squared returns) over horizons of 1, 5, 10, 20, 30, 40 and 50 days and evaluate the quality of these forecasts via their root mean squared errors (RMSEs). ALW forecasts are constructed as best linear forecasts (cf. Brockwell and Davis, 1991, chap. 5). In this approach, autoregressive forecasts are computed using a vector of optimal weights that can be obtained in an iterative fashion using the autocovariances of the process. Since we are forecasting squared returns as a proxy for volatility, we only need autocovariances of squared returns to implement this approach. These are luckily available in closed form from our moment conditions. For the GARCH model, we use conditional expectations from the ML estimates. Note that this puts our agent-based model on a disadvantage as due to its nonlinear nature, there should, in principle, be better forecasts available than the best *linear* ones. These are, however, not straightforward to compute.

Results are depicted in Table 5 where we show the RMSE for each model and forecast horizon divided by the RMSE of a naive forecast using historical volatility (so that entries smaller than 1 indicate an improvement of the model-based forecast against a static one).[3] Besides these relative RMSEs we also show the probability of the null hypothesis of equal predictive performance against the alternative of better performance of the ALW model under the Diebold–Mariano test statistics (denoted by p (DM)). Note that the complementary probabilities would give the results of the mirror-imaged tests of equal predictive performance against the alternative of better performance of the GARCH model. Overall, we see a surprisingly good performance of the ALW model that typically comes out only slightly worse than the tailor-made GARCH (1,1) volatility forecast. For the stock market data, GARCH forecasts are only significantly better in 5 out of 21 cases at the 5% confidence level, mostly at the smallest horizon (for which GARCH has one particularly tailored parameter). For gold, we only find very slightly larger RMSEs for ALW than GARCH but no significant differences at any forecast horizon. For the CHF/EUR, both models have mostly RMSEs above 1 and, thus, perform worse than historical volatility. For USD/EUR and YEN/USD results resemble those of the stock market: Both forecasts show improvements against historical volatility, but those of the GARCH model are more pronounced and significantly better at short horizons.

To give some visual impression of the typical out-of-sample performance of both models, Fig. 4 depicts the one-period ahead predictions for the S & P 500 squared returns together with the empirical series. As one can see, ALW shows more persistence of its predictions than GARCH, while the later shows stronger short-run variation to shocks. Forecasts from both models can differ to quite some extent at times so that it might be promising to explore their complementarities via forecast combinations. Motivated by this observation, we have explored the question whether GARCH and ALW could be combined to provide superior forecasts than those from single models. The last three columns of Table 4 show the outcome of a standard test of forecast encompassing along the lines of Harvey et al. (1998). The fourth column of Table 4 exhibits the slope parameter λ in the forecast encompassing regression:

$$e_{1,t} = \lambda(e_{1,t} - e_{2,t}) + \epsilon_t \tag{24}$$

with $e_{1,t}$ and $e_{2,t}$ the errors of the forecasts from the GARCH and ALW model, respectively. One, thus, tests the null hypothesis $H_0 : \lambda = 0$ which means that the GARCH model encompasses the ALW model. Rejection of H_0, i.e. estimates of λ significantly different from zero indicates that the ALW model contributes useful information to the forecast problem in question on top of what the GARCH model already contributes. The fifth column of Table 4 gives the standard error of λ (allowing to access significance) and the last column shows the performance of optimally combined forecasts from GARCH and ALW ($f_{1,t}$ and $f_{2,t}$):

$$f_t^* = (1-\lambda)f_{1,t} + \lambda f_{2,t}. \tag{25}$$

[2] The expression is given as follows: rel.var. $= 1 - \sigma_f^2/\sigma_r^2 = 1 - \sigma_f^2/(\sigma_f^2 + 2b/(b+2a)(1-\exp[-2a]))$.

[3] By 'historical volatility' is meant the mean of squared returns over the in-sample period.

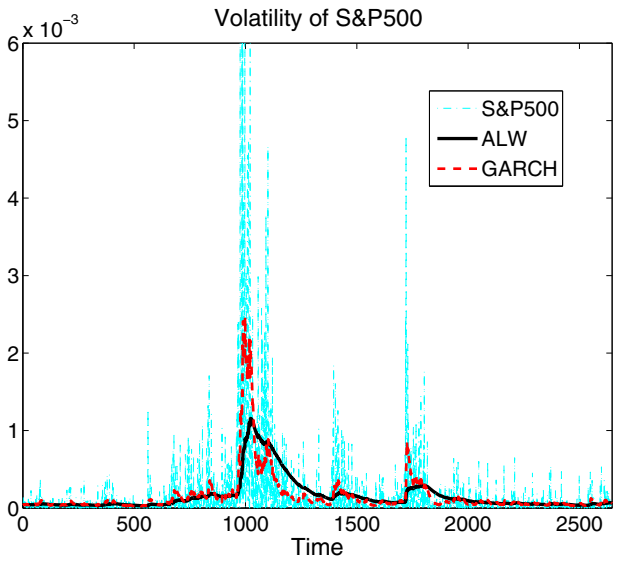

Fig. 4. Forecasts for S & P 500 Volatility. Note: The figure shows squared returns of S & P 500 over the out-of-sample period together with 1-period forecasts from the GARCH and ALW models.

As it turns out, ALW adds value at all lags for the Nikkei, at the higher forecast horizons for USD/EUR, and YEN/USD, and the lower ones for the CHF/EUR and again at most lags for gold. For the S & P 500 and the DAX, the behavioral model only makes a significant contribution at the one or two lowest horizons.

The higher persistence of the ALW forecasts underlines the proximity of this model to processes with long memory. As pointed out by Alfarano and Lux (2007) for a closely related model, the switching between different moods of market participants leads to a phenomenology of the resulting dynamics that mimics long-range dependence despite the Markovian nature of the process.

6. Conclusions

In this paper, we have explored the issues evolving around the estimation of agent-based asset pricing models as they have mushroomed over the last two decades. While we have concentrated on the particular example of the model by Alfarano et al. (2008), we believe that some of our findings would also be relevant for other models. Since we were able to derive analytical moment conditions, we believe that important features showed up more clearly than would have been under the additional complication of a simulated moment estimation.[4] First, we basically have available for the estimation of a univariate asset pricing model the moments that characterize the stylized facts of the empirical data: fat tails and volatility clustering. Since these features can be succinctly summarized by a small number of moments and additional ones would presumably only add largely redundant information, not too many parameters could be identified in this way. Indeed, we find that even with a maximally stripped down model with only three parameters, patterns of high autocorrelation of parameter estimates and weak identification did show up.

However, at the same time, a careful design of the estimation algorithm can be crucial for the precision of the estimates. Applying our approach to a broad selection of asset markets we find mostly structurally very similar results indicating a strong element of sentiment dynamics in the asset pricing process that, according to the model's decomposition, in most cases accounts for more than half of the overall variation of returns. We also used (presumably for the first time) an estimated behavioral model for forecasting of volatility. While we should certainly not expect too much success of a simple model like the present one in such an exercise, we find it interesting that this model indeed gets close in its performance to the seminal GARCH model, and often adds exploitable information on top of that used by the GARCH model.

We believe that the present approach should be interesting to pursue further. In particular, it should be explored whether different specifications of agent-based models exhibit similar behavior in their empirical application, or whether we could discriminate between them on the base of their capacity to match moments and forecast volatility. Indeed, different specifications need not be equivalent and could, thus, possibly provide combined forecasts that improve upon single ones.

[4] Chen and Lux (2015) compare SMM with GMM for the same model, and find that SMM is surprisingly inferior.

Appendix A

A.1. Derivation of moments in closed form

Unconditional even moments, $\mathbb{E}[x_t^n]$, for $n \geq 2$ can be obtained from the compact formula available in Alfarano et al. (2008, p. 114)

$$\mathbb{E}\left[\left(1-x^2\right)^k\right] = 2^{2k}\frac{\Gamma(2\epsilon)}{\Gamma(2\epsilon+2k)}\left(\frac{\Gamma(\epsilon+k)}{\Gamma(\epsilon)}\right)^2 \tag{26}$$

by a suitable change of the parameter k. Here we preserve the original notation of Alfarano et al. (2008) which should not be mixed with our usage of k from Section 3. Recall, $\epsilon = a/b$. Thus, for $k = 1$ we derive

$$\mathbb{E}\left[x_t^2\right] = \frac{1}{2\epsilon+1} = \frac{b}{b+2a}$$

and for $k = 2$ we obtain

$$\mathbb{E}\left[x_t^4\right] = \frac{3}{(2\epsilon+3)(2\epsilon+1)} = \frac{3b}{2a+3b}\mathbb{E}\left[x_t^2\right].$$

Additional details are available in Alfarano et al. (2008, p. 130).

In order to compute the moments $\mathbb{E}\left[z_t^2\right]$, $\mathbb{E}\left[z_t^4\right]$, and $\mathbb{E}\left[z_t^2 z_{t-h}^2\right]$, we need to spend some more efforts. Recall, $z_t = x_{t+1} - x_t$. It is possible to obtain sensible approximations of these moments by basing calculations on the Eulerian approximation of the stochastic differential equation of $\tilde{x}$ mentioned in Section 2:

$$d\tilde{x}_t = -2a\tilde{x}_t dt + \sqrt{2b\left(1-\tilde{x}_t^2\right)}dB_t, \tag{27}$$

where we have suppressed the entry $4a/N$ in the diffusion term as it will be negligible for sufficiently large N. The Eulerian approximation of Eq. (27) reads

$$\tilde{x}_{t+1} - \tilde{x}_t = -2a\tilde{x}_t\Delta t + \sqrt{2b(1-\tilde{x}_t^2)\Delta t}\eta_t, \tag{28}$$

where η_t is a standard normal variate independent of $\tilde{x}_t$ and where we fix $\Delta t \equiv 1$. It is interesting to note that diffusions of the format of Eq. (28) are known as Jacobi diffusions and have been used, among other applications, for modeling the dynamics of exchange rates within a target zone mechanism (Larsen and Sørensen, 2007).

Alfarano et al. (2008) make use of this approach and compute

$$\mathbb{E}\left[z_t^2\right] \simeq 2b\left(1-\mathbb{E}\left[x_t^2\right]\right) \tag{29}$$

$$\mathbb{E}\left[z_t^4\right] \simeq (2b)^2\mathbb{E}\left[\left(1-2x_t^2+x_t^4\right)\eta_t^4\right] \tag{30}$$

$$= 3(2b)^2\frac{4\epsilon(\epsilon+1)}{(2\epsilon+1)(2\epsilon+3)} \tag{31}$$

$$\mathbb{E}\left[z_t^2 z_{t-h}^2\right] \simeq 4b^2(1-2(2a+b))^{h-1}\left(\mathbb{E}\left[x_t^4\right] - \mathbb{E}\left[x_t^2\right]^2\right) + \mathbb{E}\left[z_t^2\right]^2. \tag{32}$$

Using these results it is then possible to compute the (approximate) autocorrelation function of the z_t^2-process at lag h as follows

$$C_{z^2}(h) = \frac{1}{4\epsilon^2+6\epsilon+3}\exp(-2bh(2\epsilon+1)), \tag{33}$$

cf. Alfarano et al. (2008, pp. 117131).

The second possibility to obtain the above moments is based directly on the Jacobi diffusion, Eq. (27), and its analytical tractability. The idea is to compute first the conditional expectations $\mathbb{E}\left[x_{t+1}^n | x_t^n\right]$ for $n = 1, 2, 3, 4$ in closed form by taking mathematical expectations on both sides of the suitably Itô-transformed variables. In particular, first the Itô rule is applied to derive dx_t^n and then expectations are taken. Solutions to these conditional expectations are available in closed form, however, they are often very lengthy and for brevity are avoided in our presentation. Details are available upon request. One source of lengthy expressions is the dependence of the higher order conditional expectations on the solutions of the lower order ones.

After obtaining solutions to the mentioned conditional expectations, the next step is to consider the polynomial expansions of z_t^2, z_t^4, and $z_t^2 z_{t-h}^2$ in terms of (powers) of x_t and x_{t+1} and take mathematical expectations of the components. For instance, consider $z_t^2 = x_{t+1}^2 - 2x_{t+1}x_t + x_t^2$ and take expectations from both sides. Note that the law of the iterated expectations applies to the middle term where we make use of the derived analytical conditional expectations. After very tedious calculations (details available upon request) we obtain the following results which we state in terms of more compact parameters $\alpha \equiv 2a$ and $\beta \equiv 2b$ and $\Delta t \equiv 1$:

$$\mathbb{E}\left[z_t^2\right] = 2\mathbb{E}\left[x_t^2\right](1 - \exp[-\alpha\Delta t]) \tag{34}$$

$$\mathbb{E}\left[z_t^4\right] = 8\mathbb{E}\left[x_t^4\right]\left(\frac{\alpha+\beta}{2\alpha+\beta} - \exp[-\alpha\Delta t] + \frac{\alpha}{2\alpha+\beta}\exp[-(2\alpha+\beta)\Delta t]\right) \tag{35}$$

$$\mathbb{E}[z_t z_{t-j\Delta t}] = 2\mathbb{E}\left[x_t^2\right](1 - \cosh[\alpha\Delta t])\exp[-\alpha\Delta t j] \tag{36}$$

$$\mathbb{E}\left[z_t^2 z_{t-j\Delta t}^2\right] = c_1 + c_2 - 2c_3 \tag{37}$$

where

$$c_1 = x_{11} - 2x_{12} + x_{13} \tag{38}$$

$$c_2 = x_{21} - 2x_{22} + x_{23} \tag{39}$$

$$c_3 = x_{31} - 2x_{32} + x_{33} \tag{40}$$

and

$$x_{11} = \exp(-(2\alpha+\beta)(j+1)\Delta t)\mathbb{E}\left[x_t^4\right] - \beta/[-(2\alpha+\beta)](1 - \exp(-(2\alpha+\beta)(j+1)\Delta t))\mathbb{E}\left[x_t^2\right] \tag{41}$$

$$x_{12} = \exp(-\alpha\Delta t)\exp(-(2\alpha+\beta)j\Delta t)\mathbb{E}\left[x_t^4\right] - \exp(-\alpha\Delta t)\beta/[-(2\alpha+\beta)](1 - \exp(-(2\alpha+\beta)j\Delta t))\mathbb{E}\left[x_t^2\right] \tag{42}$$

$$x_{13} = \exp(-(2\alpha+\beta)j\Delta t)\mathbb{E}\left[x_t^4\right] - \beta/[-(2\alpha+\beta)](1 - \exp(-(2\alpha+\beta)j\Delta t))\mathbb{E}\left[x_t^2\right] \tag{43}$$

$$x_{21} = \exp(-(2\alpha+\beta)j\Delta t)\mathbb{E}\left[x_t^4\right] - \beta/[-(2\alpha+\beta)](1 - \exp(-(2\alpha+\beta)j\Delta t))\mathbb{E}\left[x_t^2\right] \tag{44}$$

$$x_{22} = \exp(-\alpha\Delta t)\exp(-(2\alpha+\beta)(j-1)\Delta t)\mathbb{E}\left[x_t^4\right] - \exp(-\alpha\Delta t)\beta/[-(2\alpha+\beta)](1 - \exp(-(2\alpha+\beta)(j-1)\Delta t))\mathbb{E}\left[x_t^2\right] \tag{45}$$

$$x_{23} = \exp(-(2\alpha+\beta)(j-1)\Delta t)\mathbb{E}\left[x_t^4\right] - \beta/[-(2\alpha+\beta)](1 - \exp(-(2\alpha+\beta)(j-1)\Delta t))\mathbb{E}\left[x_t^2\right] \tag{46}$$

$$\begin{aligned} x_{31} = {} & \exp(-(2\alpha+\beta)j\Delta t)\exp(-3(\alpha+\beta)\Delta t)\mathbb{E}\left[x_t^2\right] \\ & + 3\beta/(-\alpha+3(\alpha+\beta))\exp(-(2\alpha+\beta)j\Delta t)(\exp(-\alpha\Delta t) \\ & - \exp(-3(\alpha+\beta)\Delta t))\mathbb{E}\left[x_t^2\right] \\ & - \beta/[-(2\alpha+\beta)](1 - \exp(-(2\alpha+\beta)j\Delta t))\exp(-\alpha\Delta t)\mathbb{E}\left[x_t^2\right] \end{aligned} \tag{47}$$

$$\begin{aligned} x_{33} = {} & \exp(-(2\alpha+\beta)(j-1)\Delta t)\exp(-3(\alpha+\beta)\Delta t)\mathbb{E}\left[x_t^4\right] + 3\beta/(-\alpha+3(\alpha+\beta))\exp(-(2\alpha+\beta)(j-1)\Delta t)(\exp(-\alpha\Delta t) \\ & - \exp(-3(\alpha+\beta)\Delta t))\mathbb{E}\left[x_t^2\right] - \beta/[-(2\alpha+\beta)](1 - \exp(-(2\alpha+\beta)(j-1)\Delta t))\exp(-\alpha\Delta t)\mathbb{E}\left[x_t^2\right] \end{aligned} \tag{48}$$

$$x_{32} = \exp(-\alpha\Delta t)x_{33}. \tag{49}$$

It is easy to see where the lengthy expressions come from. Simply, there are many polynomial components, unconditional expectations of which are based on very lengthy combinations of both lower-level conditional and unconditional expectations.

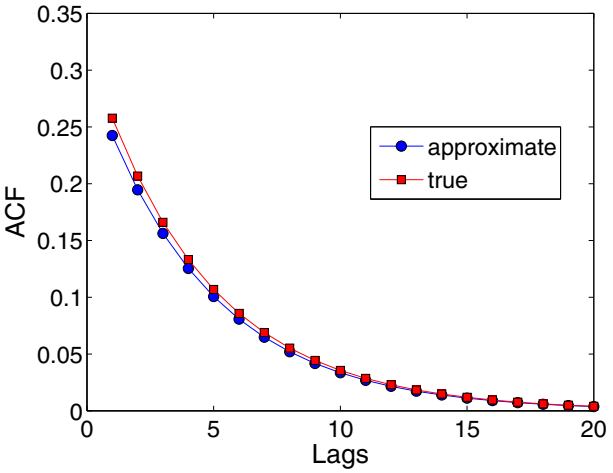

Fig. 5. 'True' and approximate autocorrelation functions of the z_t^2-process. Notes: The expressions for the 'true', $\rho_{z^2}(j)$, and approximate, $C_{z^2}(j)$, autocorrelation functions can be found in Eqs. (50) and (33), respectively. The parameters are set as $\theta^* = (a, b) = (0.005, 0.1)$. 'True' here means exact moments based on the Jacobi diffusion (27) which still is an approximation to the underlying agent-based process.

Using these results it is then possible, for instance, to compute the autocorrelation function of the z_t^2-process at lag h with $\Delta t \equiv 1$ as follows:

$$\rho_{z^2}(h) = \frac{\mathbb{E}\left[z_t^2 z_{t-h}^2\right] - \mathbb{E}[z_t^2]^2}{\mathbb{E}\left[z_t^4\right] - \mathbb{E}[z_t^2]^2}. \tag{50}$$

Thus, we obtain all the necessary building blocks for deriving the expressions for $\mathbb{E}\left[r_t^2\right]$, $\mathbb{E}\left[r_t^4\right]$, and $\mathbb{E}\left[r_t^2 r_{t-h}^2\right]$ in terms of $\mathbb{E}\left[x_t^2\right]$, $\mathbb{E}\left[x_t^4\right]$, $\mathbb{E}\left[z_t^2\right]$, $\mathbb{E}\left[z_t^4\right]$, and $\mathbb{E}\left[z_t^2 z_{t-h}^2\right]$. These moments would now be the exact counterpart of the ones obtained by Alfarano et al. (2008) via the Euler equation if Eq. (27) where the exact law of motion of the sentiment process. They are still approximate in the sense that the term $4a/N$ has been neglected in the diffusion function and that Eq. (27) is a diffusion approximation only to the 'true' underlying microscopic dynamics of agents' sentiment formation.

A.2. A comparative study of the approximating moments

From the perspective of the true agent-based model of this paper the derived moments following the two approaches are still approximations. However, among those two variants of moments the ones based on the Eulerian approximation can themselves be viewed as approximations to the 'true' moments of the Jacobi diffusion. To show their relative performance, we fix the parameters as in one calibration study of Alfarano et al. (2008, p. 119), $\theta^* = (a, b) = (0.005, 0.1)$, and compute the autocorrelations of the z_t^2-process at various lags for the two expressions in Eqs. (33) and (50).

The results are visualized for 20 lags in Fig. 5. Relative percentage deviations of the approximate ACF values from the 'true' ones for the first 10 lags are assessed in Table 6. Interestingly, visually both ACFs are in a very good agreement with each other,

Table 6
True and approximate autocorrelation functions of the z_t^2-process.

Lag h	$\rho_{z^2}(h)$	$C_{z^2}(h)$	Relative % difference
1	0.2576	0.2425	−5.8970
2	0.2068	0.1946	−5.8970
3	0.1659	0.1561	−5.8970
4	0.1332	0.1253	−5.8970
5	0.1069	0.1006	−5.8970
6	0.0858	0.0807	−5.8970
7	0.0688	0.0648	−5.8970
8	0.0552	0.0520	−5.8970
9	0.0443	0.0417	−5.8970
10	0.0356	0.0335	−5.8970

Notes: The expressions for the 'true', $\rho_{z^2}(j)$, and approximate, $C_{z^2}(j)$, autocorrelation functions can be found in Eqs. (50) and (33), respectively. The parameters are set as $\theta^* = (a, b) = (0.005, 0.1)$. 'True' here means exact moments based on the Jacobi diffusion (27) which still is an approximation to the underlying agent-based process.

however, we observe virtually constant relative undervaluation at about six percent of the approximate ACF to the 'true' one. Nevertheless, the quality that is clearly obtained by the Euler approximation of the highly nonlinear Jacobi diffusion for the ACF is striking.

Another robust finding of our investigation is that approximate moments tend to consistently overestimate kurtosis, however, this overvaluation is very small (almost zero) and, therefore, can be tolerated.

To summarize, we observe that both the simple Euler approximation and the much more involved derivation of exact moments from the diffusion (27) lead to almost the same numerical values. Small deviations are present but seem tolerable. While we have applied the more precise moment conditions based on the Jacobi diffusion in the main text, additional experiments confirmed that outcomes of GMM estimation are always very similar under both alternatives.

A.3. Monte Carlo results for the exact discretization

In addition to the simulation study provided in the main text we have also conducted *exact* simulations of the agent based model with 100 agents and the same underlying parameters. The agent-based sentiment dynamics can be simulated exactly as a system of iscrete events. The Poisson transition rates defined in Eqs. (1) and (2) in the main text imply that agents' changes of opinion occur over time with an exponential distribution for the time intervals between subsequent changes. While the opinion formation is characterized by an exponential distribution for all agents, its parameter differs between the currently optimistic and pessimistic ones depending on the different degrees of pressure exerted on them by the tendency to follow the majority. Despite this heterogeneity, one can get an exact sample from this process by taking into account the known fact, that the minimum of independently and exponentially distributed exponential variates also follows an exponential distribution, with its parameter equal to the sum of individual parameters, i.e. $\lambda = n_t\pi_{\downarrow,t} + (N - n_t)\pi_{\uparrow,t}$. Hence, using such exponential draws, we can determine the next instant for the change of opinion of any one agent. The fractions $n_t\pi_{\downarrow,t}/\lambda$ and $(N - n_t)\pi_{\uparrow,t}/\lambda$, then determine which type of change we execute. The resulting composition of the population is recorded and its configuration at integer time

Table 7
Monte Carlo results for GMM estimation of ALW Model under exact discretization.

True:	0.3	1.4	30	0.3	1.4	30	0.3	1.4	30
	GMM1			GMM2			GMM3		
	a	b	σ_f	a	b	σ_f	a	b	σ_f
T = 5000									
Mean	0.444	1.144	28.463	0.363	1.242	28.308	0.358	1.319	28.650
FSSE	0.265	0.498	5.121	0.187	0.316	5.655	0.182	0.323	6.799
RMSE	0.301	0.560	5.341	0.197	0.353	5.896	0.191	0.333	6.924
T = 10,000									
Mean	0.410	1.183	28.045	0.304	1.356	29.805	0.315	1.415	29.591
FSSE	0.201	0.507	5.239	0.110	0.296	4.757	0.133	0.279	5.996
RMSE	0.229	0.551	5.586	0.109	0.299	4.755	0.134	0.279	6.003
T = 20,000									
Mean	0.421	1.109	28.307	0.278	1.488	31.191	0.288	1.526	30.928
FSSE	0.216	0.480	5.384	0.083	0.210	3.491	0.105	0.185	4.676
RMSE	0.247	0.561	5.638	0.086	0.227	3.685	0.106	0.223	4.761
True:	1.4	0.3	30	1.4	0.3	30	1.4	0.3	30
	GMM1			GMM2			GMM3		
	a	b	σ_f	a	b	σ_f	a	b	σ_f
T = 5000									
Mean	0.884	0.686	27.779	0.925	0.447	27.743	1.031	0.446	27.408
FSSE	0.431	0.567	1.965	0.244	0.011	1.134	0.213	0.011	0.642
RMSE	0.672	0.685	2.964	0.534	0.148	2.525	0.426	0.147	2.670
T = 10,000									
Mean	0.971	0.660	27.208	0.988	0.447	27.589	1.057	0.447	27.336
FSSE	0.396	0.549	2.856	0.209	0.009	0.897	0.138	0.009	0.451
RMSE	0.583	0.656	3.992	0.462	0.148	2.572	0.370	0.147	2.702
T = 20,000									
Mean	1.014	0.620	27.173	1.029	0.447	27.465	1.065	0.447	27.307
FSSE	0.338	0.510	2.245	0.168	0.006	0.673	0.073	0.006	0.255
RMSE	0.513	0.601	3.608	0.407	0.147	2.623	0.342	0.147	2.705

Notes: The table shows the means, finite sample standard errors (FSSE) and root-mean squared errors (RMSE) of 400 replications of each scenario. Estimated parameters are multiplied by 10^3 for better readability. GMM1 stands for a standard GMM estimation, while in GMM2 the estimation has been initiated with the inverse of the variance–covariance matrix of the test data as the weighting matrix in the first step of the estimation. In GMM3, single autocovariances have been replaced by sums of autocovariances.

steps serves to determine discretely observed returns as defined in Eq. (7). We use this discrete-event simulation to perform a Monte Carlo experiment along the lines of the one reported in Table 2 for the diffusion approximation. The estimation results are summarized in Table 7. All results are very close to those reported in the main text which confirm that (i) the Jacobi diffusion closely approximates the aggregate dynamics of the micro-level sentiment dynamics, and (ii) the moment conditions derived from the diffusion approximation are also sufficiently close to the unknown 'true' moments of the agent-based model to allow GMM estimation of its parameters at the same level of accuracy as with the Jacobi diffusion itself.

References

Alfarano, S., Lux, T., 2007. A noise trader model as a generator of apparent power laws and long memory. Macroecon. Dyn. 11, 80–101.
Alfarano, S., Lux, T., Wagner, F., 2005. Estimation of agent-based models: the case of an asymmetric herding model. Comput. Econ. 26, 19–49.
Alfarano, S., Lux, T., Wagner, F., 2008. Time variation of higher moments in a financial market with heterogeneous agents: an analytical approach. J. Econ. Dyn. Control. 32, 101–136.
Amilon, H., 2008. Estimation of an adaptive stock market model with heterogeneous agents. J. Empir. Financ. 15, 342–362.
Aoki, M., 2002. Modeling Aggregate Behavior and Fluctuations in Economics. University Press, Cambridge.
Bollerslev, T., 1986. A generalized autoregressive conditional heteroskedasticity. J. Econ. 31, 307–327.
Brock, W.A., Hommes, C.H., 1998. Heterogeneous beliefs and bifurcation routes to chaos in a simple asset pricing model. J. Econ. Dyn. Control. 22, 1235–1274.
Chen, Z., Lux, T., 2015. Estimation of sentiment effects in financial markets: a simulated method of moments approach. Working Paper. University of Kiel,
Cont, R., Bouchaud, J.P., 2000. Herd behavior and aggregate fluctuations in financial markets. Macroecon. Dyn. 4, 170–196.
De Grauwe, P., Dewachter, H., Embrechts, M.J., 1993. Exchange Rate Theory: Chaotic Models of Foreign Exchange Market. Blackwell, Oxford.
Ethier, S., Kurtz, T., 1986. Markov Processes. Wiley, New York.
Franke, R., Westerhoff, F., 2011. Estimation of a structural volatility model of asset pricing. Comput. Econ. 38, 53–83.
Franke, R., Westerhoff, F., 2012. Structural stochastic volatility in asset pricing dynamics: estimation and model contest. J. Econ. Dyn. Control. 36, 1193–1211.
Franke, R., Westerhoff, F., 2014. Why a simple herding model may generate the stylized facts of daily returns: explanation and estimation. J. Econ. Interac. Coord. 1–34.
Gilli, M., Winker, P., 2003. A global optimization heuristic for estimating agent based models. Comput. Stat. Data Anal. 42 (3), 299–312.
Hall, A.R., 2005. Generalized Method of Moments. Oxford University Press, Oxford.
Hansen, L.P., 1982. Large sample properties of Generalized Method of Moments estimators. Econometrica 50, 1029–1054.
Harvey, D., Leybourne, S., Newbold, P., 1998. Tests for forecast encompassing. J. Bus. Econ. Stat. 16, 254–259.
Hommes, C., 2006. Heterogeneous agent models in economics and finance. In: Tesfatsion, L. (Ed.), Agent-Based Computational Economics, Handbook of Computational Economics, Vol. 2. North-Holland. pp. 1109–1186.
Jang, T.S., 2013. Identification of social interaction effects in financial data. Comput. Econ. 45 (2), 207–238.
Kirman, A., 1993. Ants, rationality, and recruitment. Q. J. Econ. 108 (1), 137–156.
Kirman, A.P., 1991. Epidemics of Opinion and Speculative Bubbles in Financial Markets in Money and Financial Markets. In: Taylor, M. (Ed.), . Macmillan, London.
Larsen, K., Sørensen, M., 2007. Diffusion models for exchange rates in a target zone. Math. Financ. 17 (2), 285–306.
LeBaron, B., 2006. Agent-based computational finance. In: Tesfatsion, L. (Ed.), Agent-Based Computational Economics, Handbook of Computational Economics, Vol. 2. North-Holland. pp. 1187–1233.
LeBaron, B., Arthur, W.B., Palmer, R., 1999. The time series properties of an artificial stock market. J. Econ. Dyn. Control. 23, 1487–1516.
Lux, T., 1995. Herd behaviour, bubbles and crashes. Econ. J. 105, 881–896.
Lux, T., 1998. The socio-economic dynamics of speculative markets: interacting agents, chaos, and the fat tails of return distributions. J. Econ. Behav. Organ. 33, 143–165.
Lux, T., 2008. Stochastic behavioral asset pricing models and the stylized facts. In: Hens, T., Schenk-Hoppé, K. (Eds.), Handbook of Financial Markets: Dynamics and Evolution. Amsterdam, North-Holland.
Lux, T., Marchesi, M., 1999. Scaling and criticality in a stochastic multi-agent model of a financial market. Nature 397, 498–500.
Lux, T., Schornstein, S., 2005. Genetic algorithms as an explanation of stylized facts of foreign exchange markets. J. Math. Econ. 41, 169–196.
McManus, D., 1992. How common is identification in parametric models? J. Econ. 53, 5–23.
Samanidou, E., Zschischang, E., Stauffer, D., Lux, T., 2007. Agent-based models of financial markets. Rep. Prog. Phys. 70, 409–450.
Shiller, R.J., 1981. Do stock prices move too much to be justified by subsequent changes in dividends? American Economic Review 71 (3). 421–436.